JSST 2022

Numerical Experiments of Swelling Objects Interacting with Newtonian Fluids

Niku Guinea[1,*], Daisuke Toriu[2], Satoru Ushijima[2]

[1]Department of Civil and Earth Resources Engineering, Graduate School of Engineering, Kyoto University
[2]Academic Center for Computing and Media Studies, Kyoto University

[*]guinea.niku.25w@st.kyoto-u.ac.jp

Abstract.

Deformable swelling particles interacting with Newtonian fluid was computed using the combination of direct-forcing immersed boundary method and mass-spring model. The swelling of the object was simulated by changing the natural lengths of the spring models. In addition, the solid-solid interaction is treated by utilizing the distinct element method. Two cases of interaction between multiple swelling objects and Newtonian fluid are proposed. As a result, it was shown that the basic behaviors of the swelling-deformable objects are reasonably calculated with the present method.

Keywords: Fluid-solid interaction, Swelling, Deformable object, Immersed boundary method, Mass-spring model

1. Introduction

The interactions between Newtonian fluids and swelling bodies with deformable properties are introduced in this study. The combination of direct-forcing immersed boundary method (DF/IB) [1] and mass-spring model (MSM) [2] is proposed for the computation of the interactions of fluid and deformable solid. In addition, the swelling of the object is proposed by changing the natural lengths of the spring models. The solid-solid interaction is treated by setting CDS (contact detection sphere) along the solid boundary to detect particle collisions for DEM computation. The Lagrangian (mass) points used in the MSM-DF/IB computations share the same points for the placement of CDS used in the particle collisions. Furthermore, as the swelling computation is utilizing the natural spring length used in MSM, the coupling of the three methods in one computation is fairly easy.

2. Numerical method

The fluid is assumed to be incompressible, and the momentum equations are given by

$$\frac{\partial u_i}{\partial t} + \frac{\partial (u_i u_j)}{\partial x_j} = -\frac{1}{\rho_f}\frac{\partial p}{\partial x_i} + \nu \frac{\partial^2 u_i}{\partial x_j^2} + f_i + \lambda_i, \tag{1}$$

where u_j is the velocity component in x_j direction in two-dimensional Cartesian coordinates, t is time, x_i is the component of the Cartesian coordinate system, ρ_f is density, ν is kinematic viscosity, and p is pressure. In addition, u_i is the velocity component, f_i and λ_i are the external and fluid-solid interaction forces in x_i direction.

For the details of the computation of MSM-DF/IB, the reader are referred to the detailed explanation by Guinea et al. [3]. The swelling of objects is calculated by increasing the natural spring length used in the mass-spring model. As the value of the natural spring length increases, the restoring force acts on the mass points and the distances between them also increases. The swelling scheme is applied to the computation of the swelling of a single hydrogel particle and gives a good agreement when compared to the experiment as introduced in Guinea et al. [4]. In the proposed method, it is assumed that the volume increase of the object is equal to the absorbed fluid. Additionally, for simplicity, the density of the object is assumed to be constant in this study.

3. Applications

3.1. Sedimentation of a single particle in fluid

A swelling particle with initial diameter $D_0 = 0.25$ and density $\rho_s = 1.25$ is set inside a 2×8 area. The particle is dropped from the initial position of $(1, 6)$ and falls freely with the gravity acceleration of -980. The particle swells from $t = 0.30$ until the maximum diameter $D_{max} = 0.30$. The surrounding sides are treated as non-slip boundaries. The fluid density ρ_f and kinematic viscosity ν are 1.0 and 0.1 respectively. The spring constant and coefficient of restitution of mass-spring model k_s and e_s are 4×10^6 and 0.5. The number of fluid cells used in the computation is 200×800, the number of Lagrangian points N_l is 70, and Δt is 5×10^{-3} The calculated particle velocity in y direction is observed and compared with the case of sedimentation of non-swelling particle with $D = 0.25$ and $D = 0.30$.

The changes of the particle diameter and the time history of the particle velocities can be seen on Fig. 1. The computation shows reasonable results between the three computations. On the non-swelling particles, the terminal velocity of the particle with smaller diameter (blue line) is smaller, causing the particle to reach the bottom side later than the particle with larger diameter (green line). The red line represents the velocity of the swelling particle. Prior to $t = 0.3$, the velocity of the swelling particle is equal to the blue line where the particle is identical in size. Afterward, the particle starts to swell and the velocity gradually reaches the green line. In addition, due to the increase of the particle velocity on the swelling particle, it reaches the bottom side before the particle with $D = 0.25$ and after the particle with $D = 0.3$.

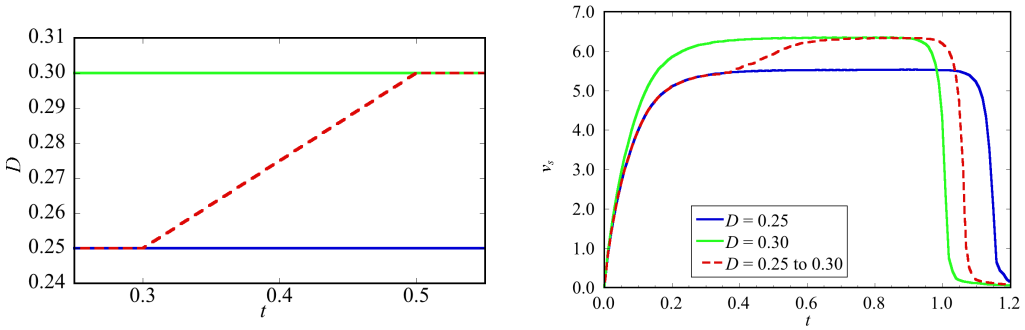

(a) Changes of particles diameter

(b) Time histories of particle velocity

Figure 1: Comparison of diameter and particle velocities between the three cases

3.2. Multiple objects transported in two-sided lid-driven cavity flow

Multiple deformable solid particles with various sizes are arranged inside the 2D computational area filled with fluid as it can be seen on Figs. 2 (a) and 3 (a). The computational area is filled with fluid with kinematic viscosity $\nu = 0.01$ and fluid density $\rho_f = 1.0$. The surrounding walls are treated as non-slip boundaries. The top and bottom walls move in horizontal direction with velocities $u_{top,1} = 1.0$, $u_{top,2} = 0.0$, $u_{bottom,1} = -1.0$, and $u_{bottom,2} = 0.0$. The Reynolds number Re is 100. 16 particles with the initial diameter D_0 varied between 0.1 and 0.15 with density $\rho_s = 1.5$ are set up on the computational area. The spring stiffness k_s of the particles are set between 0.56 and 0.88, with the coefficient of restitution $e_s = 1.0$. For the DEM computation, the values of spring constant $k_{D,n}$ in normal direction is 1.0×10^7. Tangential contact forces is assumed to be 0 in this computation. The coefficient of restitution e_D of DEM computation is 1.0, and the radius of the contact detection spheres is $0.167D$. The number of fluid cells used is 100×100, while the number of mass (Lagrangian) points N_l is 21. In addition, the time increment Δt is 1.0×10^{-4}. Two cases are computed in this study. In both cases, velocities on top and bottom walls are stopped after $t = 10$. Non-swelling particles are introduced in the first case, while swelling particles are on the second case. The particles on the second case are set to swell linearly with the slope of 3×10^{-3} until the maximum size D_{max} of $1.5D_0$.

Figures 2 and 3 show the computation results on the non swelling and swelling particles. The black lines represent the line connecting the mass (Lagrangian) points, and red lines represent the line connecting the outer side of the contact detection spheres. Additional lines are drawn connecting the surface and the center of the object to help observe rotation on the particles. Due to the movement of the top and bottom wall, deformations can be observed especially closer to the moving top and bottom wall where velocity is higher and when the solid-solid and solid-wall contacts occur. After the velocities are stopped on $t = 10$, we can see the particles move only with their remaining speed and finally stopped. The trajectories of the center points of the particles for $10 \leq t \leq 20$ can be seen on Fig. 4. It can be observed that the non-swelling particles are moving further than the swelling particles after the velocities are stopped. In addition, after the velocity is stopped, the particles on the second case are still swelling. As a result, the particles push each other, causing slight movement as it can be observed on the discontinuous lines on Fig. 4 (b).

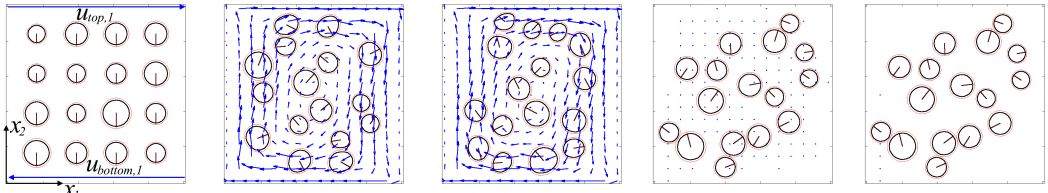

(a) $t = 0$ (b) $t = 5$ (c) $t = 10$ (d) $t = 15$ (e) $t = 20$

Figure 2: Computation of non-swelling particles

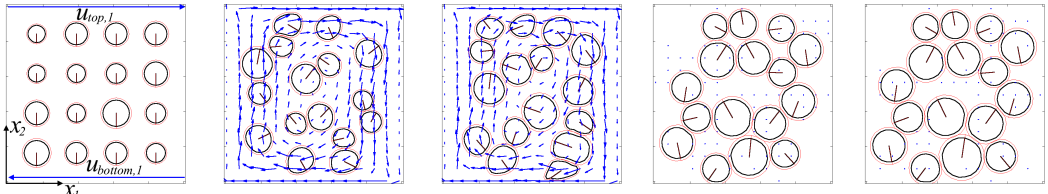

(a) $t = 0$ (b) $t = 5$ (c) $t = 10$ (d) $t = 15$ (e) $t = 20$

Figure 3: Computation of swelling particles

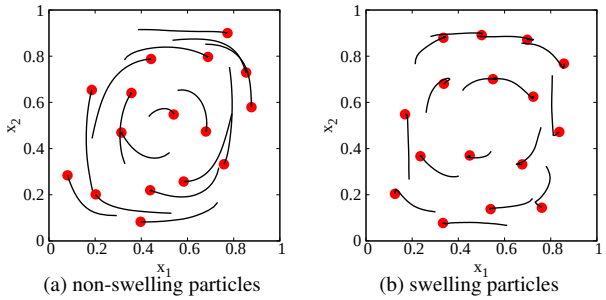

(a) non-swelling particles (b) swelling particles

Figure 4: Trajectories of non-swelling and swelling particles for $10 \leq t \leq 20$ (red points mark the position of the particles at $t = 20$)

References

[1] M. Uhlmann : An immersed boundary method with direct forcing for the simulation of particulate flows, *J. Comput. Phys.*, vol. 209, 448–476, (2005)

[2] D. Terzopoulos, J. Platt, A. Barr, K. Fleischer : Elastically deformable models, *ACM Siggraph Computer Graphics*, vol. 21, 205–214, (1987)

[3] N. Guinea, D. Toriu, S. Ushijima : Computational method for interactions between deformable objects and fluid flows using immersed boundary method and mass spring model, *Transaction of Japan Society for Simulation Technology*, (2021)

[4] N. Guinea, D. Toriu, S. Ushijima : Eulerian-Lagrangian Approach for Interactions between Fluids and Multiple Deformable Swelling Objects using Mass-Spring Model, *The 25th Applied Mechanics Symposium*, 2B07-12-01, (2022)